CHEMISTRY OF MATERIALS

Article

pubs.acs.org/cm

Cyclometalated Ir(III) Complexes for High-Efficiency Solution-Processable Blue PhOLEDs

Valery N. Kozhevnikov,[†,‡] Yonghao Zheng,[†] Matthew Clough,[†] Hameed A. Al-Attar,[§] Gareth C. Griffiths,[§] Khalid Abdullah,[§] Steponas Raisys,[∥] Vygintas Jankus,[§] Martin R. Bryce,*[,†] and Andrew P. Monkman*[,§]

[†]Department of Chemistry, Durham University, Durham DH1 3LE, United Kingdom

[‡]School of Life Sciences, Northumbria University, Northumberland Road, Newcastle upon Tyne, NE1 8ST, United Kingdom

[§]Department of Physics, Durham University, Durham DH1 3LE, United Kingdom

[∥]Institute of Applied Research, Vilnius University, Saulėtekio 9-III, Vilnius LT-10222, Lithuania

Supporting Information

ABSTRACT: This article reports the systematic functionalization of FIrpic (**1**) with solubilizing alkyl groups (complexes **2**–**4**) or mesityl groups (complexes **5** and **6**). Complex **5** is shown to offer significant advantages over FIrpic (**1**) in terms of performance of sky-blue polymer-based phosphorescent organic light-emitting diodes (PhOLEDs) with a solution-processed emitting layer (λ_{max}^{EL} 477 nm for **5**). Devices with **5** doped into poly(vinylcarbazole) (PVK):OXD-7 gave a maximum luminous efficiency of 19.1 cd A^{-1} at a brightness of 5455 cd m^2 with EQE 8.7%. Optimized multilayer devices with additional TPBi and LiF layers gave 23.7 cd A^{-1} and EQE 10.4%. These data compare favorably with leading literature values for sky-blue polymer-based PhOLEDs. The enhanced performance of **5** is ascribed to three main reasons: (i) reduced concentration quenching of **5**; (ii) the higher radiative yield of **5**; and (iii) improved solubility of **5** in organic solvents. Complex **5** should find widespread use as a soluble blue phosphor for displays and lighting applications using solution processing techniques.

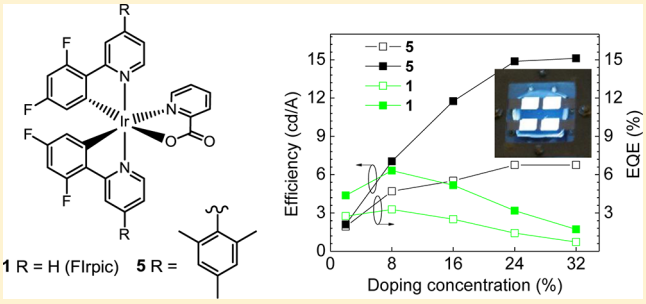

KEYWORDS: *iridium complex, phosphorescence, electroluminescence, blue emission, OLED*

INTRODUCTION

Red-green-blue (RGB) emitters with high luminous efficiency are essential for full-color organic light-emitting diode (OLED) displays[1] and solid-state lighting.[2,3] Phosphorescent cyclometalated complexes provide improved electroluminescence efficiencies by utilizing both triplet and singlet electroexcitation pathways. They have the benefits of relatively short excited state lifetimes, high photoluminescence efficiency, good color tuneability, and general thermal and electrochemical stability.[4−6] In this context, the archetypal complex is the green emitter *fac*-Ir(ppy)$_3$ (ppy = 2-phenylpyridine). For blue emission, electron-withdrawing substituents are attached to the phenyl ring of ppy ligands to decrease the HOMO energy while keeping the LUMO energy relatively unchanged.[7,8] Based on this strategy, fluorine is the most utilized substituent and the benchmark sky-blue emitter for phosphorescent OLEDs (PhOLEDs) is iridium(III) bis[4,6-(difluorophenyl)-pyridinato-*N*,*C* 2′]picolinate (FIrpic **1**) (Figure 1).[9−13] However, FIrpic suffers two major drawbacks. (i) It has poor solubility in common organic solvents; this limits the concentration at which it can be used as a dopant in solution-processed layers. (ii) FIrpic partially decomposes during vacuum deposition into PhOLED architectures with loss of the pic ligand and defluorination.[14,15] Therefore, there is a need for new phosphors that retain the blue emission and efficiency of FIrpic and have good solubility in organic solvents to enable solution processing and ink jet printing, which are the methods of choice for large-area device applications. In these processes, the molecules are not subjected to the high temperatures of vacuum deposition. The advantages of solution processing over thermal evaporation have been widely recognized.[16−20]

To address these issues, we have explored systematic functionalization of the ppy ligands of FIrpic with solubilizing alkyl groups (**2**-**4**) or mesityl groups (**5**,**6**). Structure−property relationships in the series of phosphors are established by photophysical measurements and electrophosphorescent devices with the complex doped into PVK as the solution-processed emitting layer. Complex **5** is shown to be the best material in this series, displaying the following attractive combination of properties. (i) **5** displays sky-blue electroluminescence (λ_{max}^{EL} 477 nm); (ii) solution-processed PhOLEDs of **5** using a simple solution-processed device architecture show considerably enhanced performance compared to FIrpic (**1**); (iii) reduced

Received: April 3, 2013
Revised: May 2, 2013

   dx.doi.org/10.1021/cm4010773 | *Chem. Mater.* XXXX, XXX, XXX−XXX

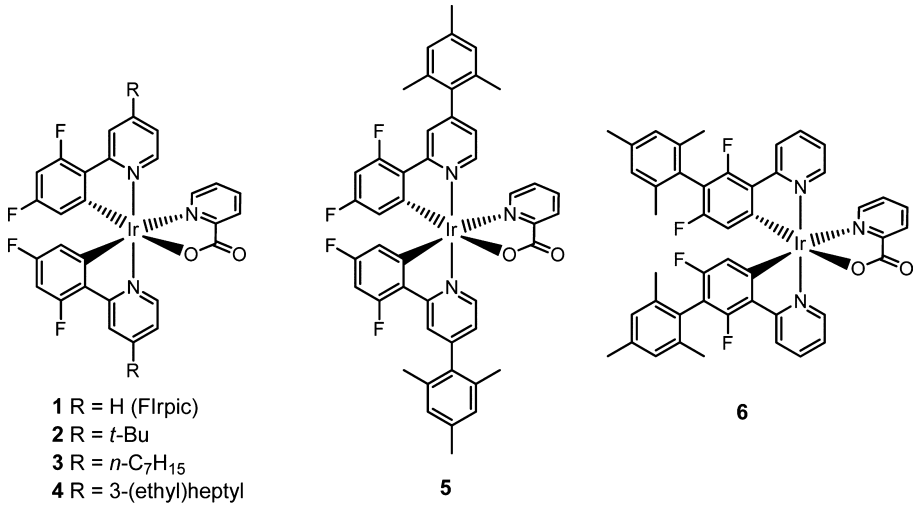

Figure 1. Structures of the iridium complexes.

concentration quenching of **5** is observed, and (iv) **5** is straightforward to synthesize and has been obtained in >1 g batches.

EXPERIMENTAL DETAILS

2-Chloro-4-(2,4,6-trimethylphenyl)pyridine (B). A mixture of 2-chloro-4-iodopyridine (**A**) (3.83 g, 16 mmol), 2,4,6-trimethylphenylboronic acid (2.62 g, 9.4 mmol), 2 M aqueous K_2CO_3 (24 mL, 48 mmol), and 1,4-dioxane (50 mL) was degassed by bubbling argon through the mixture for 15 min. Tetrakis(triphenylphosphine)-palladium(0) (554 mg, 0.48 mmol) was added, and the reaction mixture was stirred at 95 °C for 3 days, then cooled to room temperature. Toluene (50 mL) was added, and the layers were separated. The organic layer was then washed with water (2 × 30 mL) and dried over magnesium sulfate. The organic solvent was removed by rotary evaporation and the residue was purified by column chromatography (eluent ethyl acetate/hexane, 1:5 v/v). The product was then distilled using a Kugelrohr apparatus (0.6 mbar, 145 °C) to give **B** as a colorless liquid (2.37 g, 64%). ^{1}H NMR (400 MHz, $CDCl_3$): δ 8.46 (dd, J = 5.0 Hz, J = 0.7 Hz, 1H), 7.18 (dd, J = 1.4 Hz, J = 0.7 Hz, 1H), 7.07 (dd, J = 5.0 Hz, J = 1.4 Hz, 1H), 6.97 (s, 2H), 2.35 (s, 3H), 2.02 (s, 6H). ^{13}C NMR (100 MHz, $CDCl_3$): δ 153.0, 151.8, 149.7, 138.0, 134.9, 128.5, 125.2, 123.7, 21.0, 20.5. m/z (EI) (%): 230.9 (90) [M^+], 196.0 (100) [M^+−Cl]. HRMS m/z (ASAP$^+$) ($C_{14}H_{14}NCl$): calc. 231.0815, found 231.0808.

2-(2,4-Difluorophenyl)-4-(2,4,6-trimethylphenyl)pyridine (C). A mixture of **B** (340 mg, 1.47 mmol), 2,4-difluorophenylboronic acid (348 mg, 2.2 mmol), palladium(II) acetate (20 mg, 0.09 mmol), triphenylphosphine (100 mg, 0.38 mmol), and 2 M aqueous solution of sodium carbonate (3 mL, 6 mmol) in 1,2-dimethoxyethane (20 mL) was degassed by bubbling argon through the mixture for 15 min. The mixture was heated to reflux under argon atmosphere for 24 h and then cooled to room temperature. Dichloromethane (50 mL) was added, and the organic layer was separated, washed with brine (2 × 10 mL), and dried over magnesium sulfate. After removal of the solvents by rotary evaporation, the product was purified by column chromatography (eluent ethyl acetate/hexane, 1:5 v/v) to yield **C** (340 mg, 75%) as a pale yellow liquid. ^{1}H NMR (400 MHz, $CDCl_3$): δ 8.78 (dd, J = 5.0 Hz, J = 0.8 Hz, 1H). 8.10 (td, J = 8.8 Hz, J = 6.7 Hz, 1H), 7.61 (ddd, J = 2.5 Hz, J = 1.5 Hz, J = 0.9 Hz, 1H), 7.11 (dd, J = 5.0 Hz, J = 1.5 Hz, 1H), 7.05 (m, 1H), 7.00 (br s, 2H), 6.93 (ddd, J = 11.3 Hz, J = 8.8 Hz, J = 2.5 Hz, 1H), 2.37 (s, 3H), 2.08 (s, 6H). ^{13}C NMR (101 MHz, $CDCl_3$): δ 164.5, 161.9, 159.3, 152.7, 152.6, 150.0, 149.8, 137.6, 136.2, 135.2, 134.9, 132.3, 132.2, 132.2, 132.1, 128.4, 128.4, 125.3, 125.2, 123.8, 123.7, 123.5, 112.0, 111.9, 111.8, 111.7, 104.6, 104.4, 104.3, 104.1, 21.0, 20.6. HRMS m/z (ASAP$^+$) ($C_{20}H_{17}F_2N$+H): calc. 310.1407, found 310.1397.

Iridium(III)bis[2-(2,4-difluorophenyl)-4-(2,4,6-trimethylphenyl)pyridinato-N,C$^{2'}$]picolinate. Complex **5**. A mixture of **C** (340 mg, 1.1 mmol), iridium(III) chloride trihydrate (176 mg, 0.5 mmol), 2-ethoxyethanol (15 mL) and water (5 mL) was heated under reflux for 24 h. The precipitated solid was separated by filtration, washed with water and dried to give the intermediate bis(μ-Cl)dimer complex (330 mg). A mixture of this complex (330 mg), picolinic acid (240 mg), sodium carbonate (207 mg), and 2-ethoxyethanol (10 mL) was heated under reflux for 4 h. The mixture was evaporated to dryness and the product was purified by column chromatography (eluent DCM/ethyl acetate, 5:1 v/v) to afford complex **5** (215 mg, 46%) as a yellow solid. ^{1}H NMR (400 MHz, $CDCl_3$): δ 8.74 (d, J = 5.9 Hz, 1H), 8.34 (d, J = 7.8 Hz, 1H), 8.04 (s, 1H), 7.98 (s, 1H), 7.93 (td, J = 7.7, 1.5 Hz, 1H), 7.84 (dd, J = 5.0, 1.2 Hz, 1H), 7.50 − 7.34 (m, 2H), 7.06 − 6.84 (m, 5H), 6.74 (dd, J = 5.9, 1.7 Hz, 1H), 6.40 (dd, J = 5.9, 1.7 Hz, 1H), 6.36 − 6.28 (m, 1H), 5.76 (dd, J = 8.8, 2.3 Hz, 1H), 5.53 (dd, J = 8.8, 2.3 Hz, 1H), 2.29 (s, 6H), 2.09 (s, 3H), 2.05 (s, 3H), 2.03 (s, 3H), 1.91 (s, 3H). ^{19}F NMR (376 MHz, $CDCl_3$): δ −106.98 (dd, J = 19.1, 9.2 Hz), −107.87 (dd, J = 19.2, 9.2 Hz), −109.35 (t, J = 11.4 Hz), −109.90 (t, J = 11.5 Hz). m/z (MALDI+): 931.1 (100%) [M]$^+$. Calcd. for $C_{46}H_{36}N_3O_2F_4Ir$ +0.5CH_2Cl_2: C 57.37; H 3.83; N 4.32. Found: C 57.49; H 3.93; N 3.84. A scaled-up synthesis gave complex **5** (ca. 1.5 g) with no significant change (±5%) in the yield of each step from **A**.

Devices were fabricated on glass substrates coated with a 125 nm layer of indium tin oxide (ITO) with a sheet resistance of 15 Ω/□ (VisionTek). Substrates were cleaned thoroughly in acetone and isopropyl alcohol (IPA) before undergoing ozone treatment for 5 min. A ca. 75 nm layer of poly(3,4-ethylenedioxythiophene):poly-(styrenesulfonate) (PEDOT:PSS, HeraeusClevios HIL 1.5) was spin coated at 2500 rpm for 1 min and then annealed at 200 °C for 3 min to remove water. The host material poly(vinylcarbazole) (PVK) was doped with 1,3-bis[(4-*tert*-butylphenyl)-1,3,4-oxadiazolyl]phenylene (OXD-7) and with the iridium complex, blended in the ratio 100:50:12 (PVK:OXD-7:Ir complex) by weight in chlorobenzene solution at a concentration of 20 mg/mL PVK. The emissive layer was spin coated at 2500 rpm for 1 min and annealed at 120 °C for 10 min resulting in a film thickness of 76 ± 1 nm. Samples were transferred to a nitrogen glovebox where a cathode consisting of a 4 nm layer of barium followed by a 100 nm layer of aluminum was deposited by thermal evaporation at a rate of ca. 0.1 nm/s and a pressure of ca. 10^{-6} mbar. Devices were encapsulated using UV curable epoxy (DELO KATIOBOND) and a glass cover slide, exposing to UV light for 3 min. Patterning of the ITO substrate combined with masking of the cathode produced four identical pixels of 5 mm × 4 mm for each device. The resulting structure of each device was ITO/PEDOT:PSS-(73 nm)/PVK:OXD-7:Ir complex(76 nm)/Ba(4 nm)/Al(100 nm). Variations on this standard structure are stated in Table 2. TPBi and

dx.doi.org/10.1021/cm4010773 | *Chem. Mater.* XXXX, XXX, XXX−XXX

Scheme 1. Synthesis of Complex 5[a]

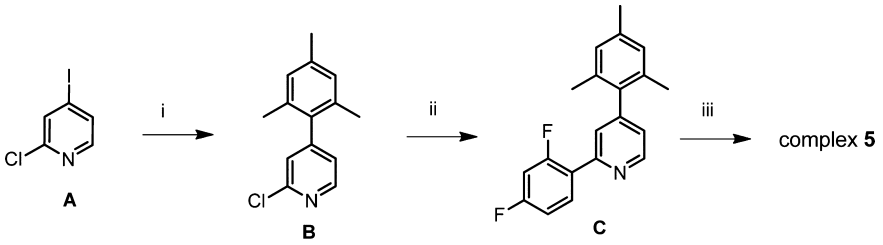

[a]Reagents and conditions: (i) 2,4,6-trimethylphenylboronic acid, aq. K_2CO_3, $Pd(PPh_3)_4$, 1,4-dioxane, 95 °C; (ii) 2,4-difluorophenylboronic acid, Na_2CO_3, $Pd(OAc)_2$, PPh_3, 1,2-dimethoxyethane, reflux; (iii) (a) $IrCl_3.3H_2O$, 2-ethoxyethanol-H_2O, reflux, (b) picolinic acid, Na_2CO_3, 2-ethoxyethanol, reflux.

LiF/Al layers were thermally evaporated using the Kurt J. Lesker Spectros II deposition system operating at 1×10^{-6} mbar.

Current–voltage data, device efficiency, brightness, and electroluminescence spectra were measured in a calibrated Labsphere LMS-100 integrating sphere. A home-written NI LabVIEW program was used to control an Agilent 6632B DC power supply, and the emission properties of the device were measured using an Ocean Optics USB4000 CCD fiber optic spectrometer. Thicknesses of the PVK:OXD-7:Ir layers were measured with a J A Woolam VASE Ellipsometer using thin films, which had been spin coated on Si/SiO_2 substrates under the same conditions as the device films. Solution state photophysical data were obtained using freshly prepared solutions of the complexes in toluene. Emission measurements were taken using thoroughly degassed solutions achieved by repeated freeze–pump–thaw cycles. All measurements were taken using quartz cuvettes with a path length of 1 cm. Absorption measurements were obtained using a Shimadzu UV-3600 UV/vis spectrometer. All emission measurements were taken using a Jobin–Yvon–Horiba SpexFluoromax 3 Spectrometer. Quantum yields were determined in degassed toluene in comparison with a standard [$Ir(ppy)_3$ = 0.4].[21] For decay measurements, the complexes were doped in an optically inert zeonex matrix, spin coated onto quartz substrates, which were subsequently mounted in a displex cryostat and evacuated with a turbo molecular pump. Samples were excited with a 450 nm dye laser pumped by a pulsed YAG laser emitting at 355 nm (from EKSPLA) at 45° angle to the substrate plane; the energy of each pulse was ca. 40 μJ per pulse. Emission was focused onto a spectrograph and detected on a sensitive gated iCCD camera (Stanford Computer Optics) with sub-nanosecond resolution. Neat films of **1** and **5** were drop-cast from chlorobenzene solutions onto sapphire substrates on a hot plate preheated at 60 °C.

RESULTS AND DISCUSSION

Figure 1 shows the structures of the complexes used in this study.

The synthesis of complex **5** is shown in Scheme 1; the syntheses of complexes **3**, **4**, and **6** are described in the Supporting Information; complex **2** has been reported previously.[22] The solubilities of complexes **2**–**6** are considerably improved compared to FIrpic (**1**). Thus, ≥25 mg of **2**–**6** are soluble in 1 mL of chlorobenzene, toluene, or 1,4-dioxane at 293 K, whereas the comparable solubility of FIrpic is ≤5 mg/mL. Complexes **2**–**6** show strong absorption bands in the 230–350 nm region (Supporting Information, Figure S1), which are assigned[9] to ligand-centered π–π^* transitions and closely resemble the absorption spectra of the free ligands. The complexes also show absorption bands with lower extinction in the range 350–400 nm, which are assigned to singlet and triplet metal-to-ligand charge-transfer (^{1}MCLT and ^{3}MLCT) states, following literature precedents.[9,23] In cyclic voltammetry experiments, complexes **1**–**6** all show a single reversible oxidation wave at very similar potentials ($E_{ox}^{1/2}$ for Ir^{3+}/Ir^{4+}, 0.84–0.87 vs ferrocene/ferrocenium couple) in acetonitrile (see Supporting Information).

The photoluminescence (PL) spectra of **1**–**6** in toluene solution are shown in Figure 2, and the data in solution and

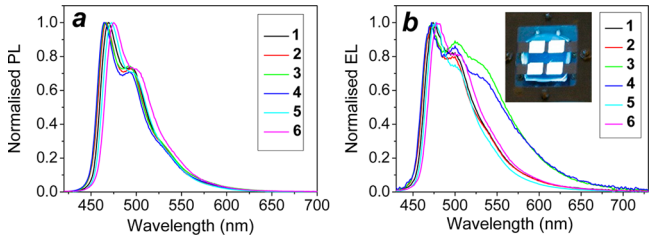

Figure 2. (a) Emission spectra of **1**–**6** in deaerated toluene solution at 293 K; λ_{exc} = 400 nm. (b) Normalized electroluminescence spectra of **1**–**6**. Inset is a photograph of a device using complex **5**. Device architecture: ITO/PEDOT:PSS/PVK:OXD-7:Ir complex (12%)/Ba/Al.

thin film are summarized in Table 1. Complexes **2**–**6** (λ_{max} 464–475 nm in PhMe; 466–476 nm in film) retain the sky-blue emission of FIrpic (λ_{max} 469 nm in PhMe; 470 nm in film). These data demonstrate the success of a key molecular design feature in **5** and **6**, namely the *ortho*-methyl groups, which twist the mesityl ring out-of-plane, thereby minimizing the extension in π–conjugation which would lead to an undesired red shift. Photoluminescence quantum yields (PLQYs) of complexes **2**–**4** and **6** are similar to that of FIrpic (**1**); however, complex **5** has a significantly higher quantum yield (Φ_{PL} 0.92). Complexes **1**, **2**, **5**, and **6** were doped in zeonex at low concentrations (0.01%), and their decay rates $1/\tau$ were recorded (Table 1). The complexes were not doped into PVK to ensure that their lifetimes were unaffected by PVK dimer quenching;[24] 0.01% concentration of complex avoids the quenching that is known to take place in films with high concentrations of Ir complexes.[25] The decay rates can be expressed as

$$1/\tau = k_r + k_{nr} \quad (1)$$

where k_r is the radiative rate, k_{nr} is nonradiative rate. In order to evaluate the effect of concentration quenching the decay rates of these complexes at high complex concentrations (12%) were also recorded:

$$1/\tau_q = k_r + k_{nr} + k_q \quad (2)$$

where k_q is the concentration quenching rate, which was evaluated by subtracting the decay rate of 0.01% complex:zeonex (eq 1) from the decay rate of 12% complex:zeonex (eq 2) (Table 2, column 3). The k_q of **1** is an order of magnitude

dx.doi.org/10.1021/cm4010773 | Chem. Mater. XXXX, XXX, XXX–XXX

Table 1. Photoluminescence Properties of 1−6 and PL decays of 1, 2, 5, and 6 in Zeonex[e]

complex	λ_{PLmax} (nm) in toluene[b]	λ_{PLmax} (nm) in film[c]	Φ_{PL} in toluene[d]	0.01% in zeonex, $k_r = 1/\tau \cdot \Phi_{PL}$, 10^6 s^{-1}	0.01% in zeonex, $1/\tau = k_r + k_{nr}$, 10^6 s^{-1}	12% in zeonex, $1/\tau_q = k_r + k_{nr} + k_q$, 10^6 s^{-1}	k_q, 10^6 s^{-1}	concn quenching efficiency, $k_q/(k_r + k_{nr} + k_q)$
FIrpic (**1**)[a]	469	470	0.54	0.41	0.75	1.12	0.37	0.33
2	467	467	0.68	0.56	0.83	0.87	0.04	0.05
3	465	467	0.66					
4	464	466	0.71					
5	473	474	0.92	1.07	1.16	1.21	0.05	0.04
6	475	476	0.55	0.39	0.71	0.81	0.10	0.12

[a]Φ_{PL} of FIrpic is reported to be 0.5−0.6 "in fluid solution";[26] 0.5 in $CHCl_3$;[27] 0.62 in CH_2Cl_2;[28] and 0.68 in MeCN.[29] [b]λ_{exc} = 400 nm. [c]Measured in PMMA film doped with 10% w/w iridium complex, λ_{exc} = 400 nm. [d]Photoluminescence quantum yield, measured in deaerated toluene solution at 293 K, λ_{exc} = 380 nm using $Ir(ppy)_3$ = 0.40 as a reference. Errors ±5%. [e]k_r is the radiative rate, k_{nr} is nonradiative rate, k_q is concentration quenching rate, $1/\tau$ is 0.01% complex doped in zeonex decay rate, $1/\tau_q$ is 12% complex doped in zeonex decay rate, Φ_{PL} is photoluminescence quantum yield, errors ±5%. PL decays were not determined for **3** and **4** as their EL is green shifted and the devices are not studied in detail in this manuscript.

Table 2. Summary of Single-Layer[a,b] and Multi-Layer[c] Device Luminescence and Efficiency Data

device no.	complex	dopant concn., wt %	$\lambda_{EL,\ max}$, nm	brightness, cd m^{-2}	turn-on voltage[e], V	η_{ext} (EQE), %	current efficiency, cd A^{-1}	power efficiency, lm W^{1-}	CIE*x,y* coordinates[f]
1[a]	**1**	12	474	1390	7	1.9	3.9	1.4	0.17, 0.38
2[a]	**2**	12	472	1440	7	3.8	7.1	2.7	0.17, 0.36
3[a]	**3**	12	472	1080	7	4.3	10.1	4.0	0.24, 0.43
4[a]	**4**	12	472	470	9	5.2	8.9	3.1	0.24, 0.41
5[a]	**5**	12	477	2290	6.5	4.6	10.1	3.6	0.16, 0.38
6[a]	**6**	12	478	1560	7	3.2	7.7	2.7	0.18, 0.43
7[b]	**5**	8	477	5455	7	8.7	19.1	6.6	0.18, 0.39
8[c]	**1**	2	472	1960	6	2.8	4.4	2.0	0.16, 0.29
9[c]	**1**	8	472	1640	5.5	3.3	6.3	3.3	0.16, 0.33
10[c]	**1**	16	472	1800	6	2.5	5.2	2.4	0.17, 0.36
11[c]	**1**	24	474	1410	6.5	1.4	3.2	1.3	0.19, 0.39
12[c]	**1**	32	478	1430	7	0.7	1.7	0.6	0.21, 0.41
13[c]	**5**	2	478	530	8	1.9	2.1	0.8	0.17, 0.25
14[c]	**5**	8	474	920	7	4.7	7.0	3.4	0.16, 0.35
15[c]	**5**	16	478	2850	5.5	5.5	11.8	5.6	0.17, 0.38
16[c]	**5**	24	478	4600	5	6.8	14.9	7.7	0.17, 0.40
17[c]	**5**	32	478	4370	5	6.8	15.1	7.7	0.17, 0.41
18[d]	**5**	20	478	4600	5	10.4	23.7	12.6	0.18, 0.40

[a]Devices 1−6: ITO/PEDOT:PSS 1.5 (73 nm)/PVK:OXD-7:Ir complex (ratio 100:50:12 w/w) (76 nm)/Ba (4 nm)/Al (100 nm). [b]Device 7: ITO/PEDOT:PSS 1.5 (75 nm)/PVK:OXD-7:complex **5** (ratio 100:37:8 w/w) (80 nm)/Ba (4 nm)/Al (100 nm). [c]Devices 8−17: ITO/PEDOT:PSS 1.5 (32 nm)/PVK:Ir complex (ca. 50 nm)/TPBi (32 nm)/LiF (0.7 nm)/Al (100 nm). [d]Device 18: ITO/PEDOT:PSS 1.1 (32 nm)/PVK:Ir complex (ca. 50 nm)/TPBi (32 nm)/LiF (0.7 nm)/Al (100 nm). [e]measured at a brightness of 10 cd m^{-2} [f]CIE coordinates measured at 12 V

higher than for complexes **2**, **5**, and **6**. Therefore, the concentration quenching efficiency for **1** is 33%, whereas for complexes **2**, **5**, and **6** it is substantially smaller (4%, 5%, 12%, respectively).

The greater concentration quenching in **1** than in **5** might be due to two reasons: (i) a reduction of intermolecular interactions in **5** arising from the bulky mesityl groups; (ii) better dispersion of 5 in the polymer matrix due to its improved solubility. To assess the roles of these two effects, the lifetimes of **1** and **5** were measured in a neat drop-cast film. The lifetimes of the neat films are not monoexponential but decay in a biexponential manner: **1** with lifetimes of 7 and 124 ns (average lifetime 109 ns); **5** with lifetimes of 30 and 242 ns (average lifetime 200 ns). This gives a concentration quenching efficiency of 0.92 for **1** and 0.77 for **5** in a neat film (see the Supporting Information, Table S1). The smaller concentration quenching in a neat film must arise due to the increased intermolecular distances in **5** in comparison with those in **1** (16% smaller concentration quenching). The difference between quenching efficiencies of **5** and **1** is greater at 12% doping ratio in zeonex (0.04 for **5** and 0.33 for **1**, Table 1; reduction in **5** by 88%). This indicates that the smaller concentration quenching in **5** in a polymer matrix mainly arises due to the improved solubility of **5**.

An initial set of PhOLEDs were fabricated by spin-coating a blend of poly(vinylcarbazole) (PVK) as the host material, OXD-7 (an electron-transporting material) and the Ir complex dissolved in chlorobenzene. Normalized EL spectra of the solution-processed devices with a simple single-active-layer structure ITO/PEDOT:PSS(73 nm)/PVK:OXD-7:Ir complex (76 nm)/Ba(4 nm)/Al(100 nm) for complexes **1**−**6** are shown in Figure 2b. The EL spectra of **2**, **5**, and **6** are all similar to that of FIrpic (**1**). The EL spectra of complexes **3** and **4** are notably broadened toward green emission, which is not observed in their PL spectra in either solution (Figure 2a) or thin film (Supporting Information, Figure S2), possibly due to the formation of an electroplex.[30]

The efficiency and luminance data of the devices are summarized in Table 2. Complexes **2**−**6** exhibit significantly higher efficiencies than FIrpic (**1**) (3.9 cd A^{-1}), under the same conditions, especially complexes **3** and **5** (10.1 cd A^{-1}). The data for the greener emitters **3** and **4** are not directly

dx.doi.org/10.1021/cm4010773 | Chem. Mater. XXXX, XXX, XXX−XXX

comparable with the other blue complexes; therefore, **3** and **4** are not discussed further. Current density, efficiency, and brightness data for complexes **1**, **2**, **5**, and **6** are shown in Figure 3, panels a–d.

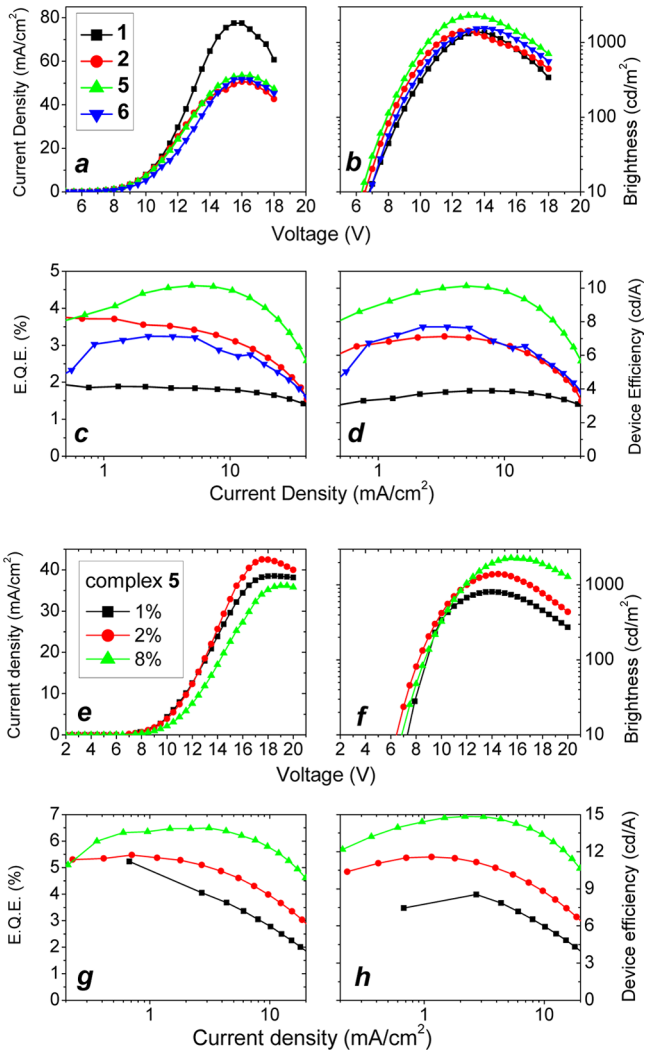

Figure 3. (a–d) Current density–voltage, efficiency, and brightness data for devices doped with complexes **1**, **2**, **5**, and **6** at 12% dopant concentration. (e–h) Data for complex **5** at dopant concentrations of 1, 2, and 8%. Device structure is stated in Figure 2b.

The significant improvement in device efficiency of **5** compared to FIrpic (**1**) can be explained by (i) improved quality of spin-coated thin films of **5**, resulting in reduced formation of aggregates of the complex in the film; (ii) reduced concentration quenching of **5** as shown by photophysical measurements of the complexes doped in the thin film. These simple solution-processed devices have a turn-on voltage between 6 and 7 V (at 10 cd m^{-2} brightness).

For the next set of single-layer devices, optimization for complex **5** was carried out by systematic variation of the dopant concentration and emissive layer thickness. Figure 3 (panels e–h) shows that the device *V*–*J* characteristics display the highest luminous efficiency (15 cd A^{-1}; EQE 6.5%) at 8% w/w dopant and an increase in the trapping efficiency as the dopant concentration increases. An increase to 19.1 cd A^{-1} and brightness 5455 cd m^{-2} corresponding to an EQE of 8.7% was obtained at 8% dopant concentration by reducing the weight% of OXD-7 in the emissive layer from 50% to 37% (Table 2; device 7). These data are shown in the Supporting Information, Figure S4.

It is known that the electron mobility plays a dominant role in determining the efficiency in FIrpic devices.[31] Consequently, high efficiency and lower turn-on voltage have generally been achieved only in more complicated device architectures involving at least one additional evaporated interlayer to optimize charge balance and confine excitons. For example, TPBi as an additional ET-HB layer,[32] arylamine derivatives as an HT layer,[33] and CsF as a cathode layer.[34,35] However, Wu et al. have reported 15.6 cd A^{-1} and 7.7% EQE for single-active-layer devices ITO/PEDOT:PSS/PVK:OXD-7:FIrpic(10%)/Ba/Al.[36] We also note that Jenekhe et al. reported that PVK-FIrpic devices with a solution-processed oligoquinoline electron-transport layer (ETL) gave efficiencies of 30.5 cd A^{-1} at a brightness of 4130 cd m^{-2} and EQE 16%.[12] In our single-emissive-layer, the low solubility of OXD-7 may increase the device leakage current and reduce device efficiency; also, the close triplet energy states of OXD-7 (2.57–2.7 eV)[37] and the emissive triplet (^{3}MLCT) energy states of the blue Ir complex (2.6 eV) may quench the emissive excitons and reduce the device efficiency.

To test if the electron transport material OXD-7 is affecting aggregation, a series of hybrid multilayer devices 8–17 (Table 2) were made without OXD-7 mixed in the active layer but instead with additional evaporated cathode interfacial layers of TPBi and LiF. The architecture is ITO/PEDOT(32 nm)/PVK doped with **1** or **5** (ca. 50 nm)/TPBi(32 nm)/LiF(0.7 nm)/Al(100 nm). The dopant concentration of **1** and **5** was varied from 2% to 32% w/w, and very different EQE and luminous efficiency dependence on dopant concentration was observed for **1** and **5**. The efficiency of **1** reaches maximum 3.3% EQE and 6.3 cd A^{-1} at 8% dopant concentration (device 9, Table 2) and then decreases (Figure 4a). In contrast, for **5** the efficiency rises with an increase of concentration and reaches a maximum of 6.8% EQE and ca. 15 cd A^{-1} at ca. 24% dopant concentration (device 16, Table 2). Further optimization of the multilayer devices with **5** as the emitter using PEDOT:PSS 1.1, instead of PEDOT:PSS 1.5, reproducibly gave efficiencies of 23 cd A^{-1} at 20% dopant (device 18, Table 2). These data are shown in the Supporting Information, Figure S5. The effects of different PEDOT:PSS conductivity on charge carrier balance[38] and OLED performance[39] have been reported. Turn-on voltages for devices 15–18 are reduced to ca. 5 V (at 10 cd m^{-2} brightness), which is typical of PVK-based PhOLEDs with an additional ETL.[12] These data confirm the increased concentration quenching of **1** in comparison with **5**, which is consistent with reduced aggregation of **5** in PVK. Indeed, the EL spectra of the PhOLEDs with FIrpic (**1**) broaden significantly with increasing dopant concentrations due to aggregation of the complex (Figure 4b). In contrast, for complex **5**, the EL spectra are essentially independent of dopant concentration (Figure 4c). These findings corroborate the photophysical investigations described above and show that FIrpic (**1**) aggregates more than **5** in PVK, a factor that contributes to the significantly higher efficiency values of PhOLEDs of **5**. The reduced aggregation of **5** is probably caused by the additional steric bulk of the mesityl substituents.

dx.doi.org/10.1021/cm4010773 | *Chem. Mater.* XXXX, XXX, XXX–XXX

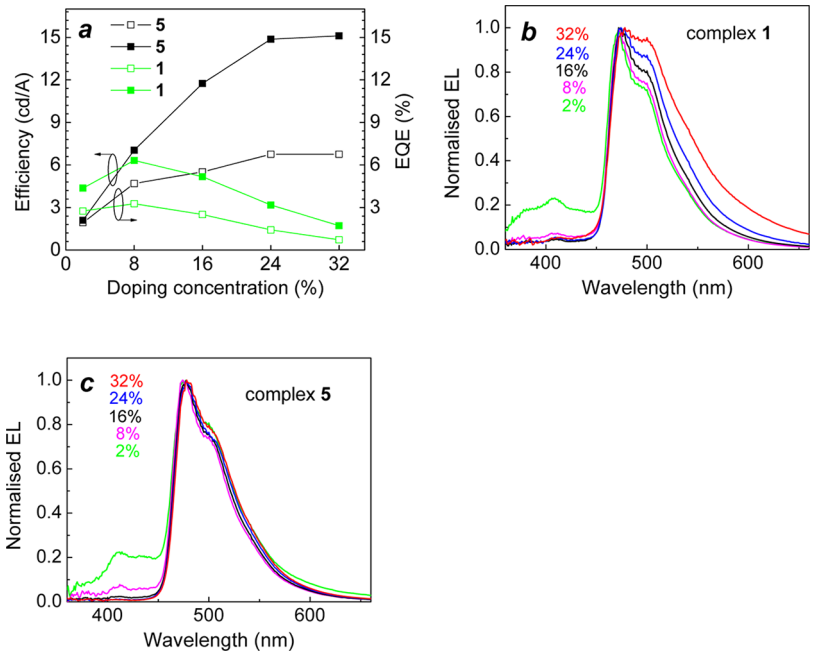

Figure 4. (a) Device efficiency data (EQE and cd A^{-1}) as a function of dopant concentration of complexes **1** and **5**. Device architecture: ITO/PEDOT:PSS 1.5(32 nm)/PVK doped with **1** or **5** (ca. 50 nm)/TPBi(32 nm)/LiF (0.7 nm)/Al(100 nm). (b) EL spectra of the device with **1** at different dopant concentrations. (c) EL spectra of the device with **5** at different concentrations.

CONCLUSIONS

In summary, a series of Ir complexes has been synthesized and studied as sky-blue dopants in solution-processed PhOLEDs. In comparative studies, complex **5** outperforms the benchmark complex FIrpic (**1**) and the other complexes **2**–**4** and **6**. Optimized single-active-layer devices with **5** doped into PVK:OXD-7 gave a maximum luminous efficiency of 19.1 cd A^{-1} at a brightness of 5455 cd m^2 with EQE 8.7%. Optimized multilayer devices with additional TPBi and LiF layers gave 23.7 cd A^{-1} and EQE 10.4%. These data compare very favorably with leading literature values for sky-blue polymer-based PhOLEDs.[12,29,30] The successful molecular design feature in **5** is the attachment of mesityl substituents to C(4) of the pyridyl ring of the ppy ligands. The *ortho*-methyl groups twist the ring out-of-plane, thereby minimizing the extension in π–conjugation and retaining the blue emission. The superiority of complex **5** over the benchmark complex FIrpic (**1**) and the other complexes studied is ascribed to three main reasons: (i) reduced concentration quenching of **5**; (ii) the higher radiative yield of **5**; and (iii) improved solubility of **5** in organic solvents. The synthesis of **5** is straightforward. Therefore, **5** should find widespread use in displays and lighting applications using solution processing techniques, without sacrificing device efficiency compared to vacuum deposited blue phosphor layers.

ASSOCIATED CONTENT

Supporting Information

Synthetic details, spectroscopic, solution electrochemical, and device data. This material is available free of charge via the Internet at http://pubs.acs.org.

AUTHOR INFORMATION

Corresponding Author

*E-mail: m.r.bryce@durham.ac.uk (M.R.B.); a.p.monkman@durham.ac.uk (A.P.M.).

Notes

The authors declare no competing financial interest.

ACKNOWLEDGMENTS

The authors thank EPSRC, the U.K. Technology Strategy Board (TSB) and Thorn Lighting for funding under the TOPLESS project.

REFERENCES

(1) *Organic Light-Emitting Devices*; Müllen, K.; Scherf, U., Eds.; Wiley-VCH: Weinheim, Germany, 2006.
(2) Kamtekar, K. T.; Monkman, A. P.; Bryce, M. R. *Adv. Mater.* **2010**, *22*, 572–582.
(3) Beaupré, S.; Boudrealt, P. L. T.; Leclerc, M. *Adv. Mater.* **2010**, *22*, E6–E27.
(4) Baldo, M. A.; O'Brien, D. F.; You, Y.; Shoustikov, A.; Sibley, S.; Thompson, M. E.; Forrest, S. R. *Nature* **1998**, *395*, 151–154.
(5) Holder, E.; Langeveld, B. M. W.; Schubert, U. S. *Adv. Mater.* **2005**, *17*, 1109–1121.
(6) Xiao, L.; Chen, Z.; Qu, B.; Luo, J.; Kong, S.; Gong, Q.; Kido, J. *Adv. Mater.* **2011**, *23*, 926–952.
(7) Ragni, R.; Plummer, E. A.; Brunner, K.; Hofstraat, J. W.; Babudri, F.; Farinola, G. M.; Naso, F.; De Cola, L. *J. Mater. Chem.* **2006**, *16*, 1161–1170.
(8) Baranoff, E.; Curchod, B. F. E.; Monti, F.; Steimer, F.; Accorsi, G.; Tavernelli, I.; Rothlisberger, U.; Scopelliti, R.; Grätzel, M.; Nazeeruddin, M. K. *Inorg. Chem.* **2012**, *51*, 799–811.
(9) Lamansky, S.; Djurovich, P.; Murphy, D.; Abdel-Razzaq, F.; Adachi, C.; Burrows, P. E.; Forrest, S. R.; Thompson, M. E. *J. Am. Chem. Soc.* **2001**, *123*, 4304–4312.
(10) Rausch, A. F.; Thompson, M. E.; Yersin, H. *Inorg. Chem.* **2009**, *48*, 1928–1937.
(11) Chen, S.; Tan, G.; Wong, W.-Y.; Kwok, H.-S. *Adv. Funct. Mater.* **2011**, *21*, 3785–3793.
(12) Ahmed, E.; Earmme, T.; Jenekhe, S. A. *Adv. Funct. Mater.* **2011**, *21*, 3889–3899.
(13) Ho, C.-L.; Chi, L.-C.; Hung, W.-Y.; Chen, W.-Y.; Lin, Y.-C.; Wu, H.; Mondal, E.; Zhao, G.-J.; Wong, K.-T.; Wong, W.-Y. *J. Mater. Chem.* **2012**, *22*, 215–224.

(14) Sivasubramaniam, V.; Brodkorb, F.; Hanning, S.; Loebl, H. P.; van Elsbergen, V.; Boerner, H.; Scherf, U.; Kreyenschmidt, M. *J. Fluorine Chem.* **2009**, *130*, 640−649.
(15) Sivasubramaniam, V.; Brodkorb, F.; Hanning, S.; Loebl, H. P.; van Elsbergen, V.; Boerner, H.; Scherf, U.; Kreyenschmidt, M. *Cent. Eur. J. Chem.* **2009**, *7*, 836−845.
(16) Zhong, C.; Duan, C.; Huang, F.; Wu, H.; Cao, Y. *Chem. Mater.* **2011**, *23*, 326−340.
(17) Arias, A. C.; MacKenzie, J. D.; McCulloch, I. *Chem. Rev.* **2010**, *110*, 3−24.
(18) Wu, H.; Zhou, G.; Zou, J.; Ho, C.-L.; Wong, W.-Y.; Yang, W.; Cao, Y. *Adv. Mater.* **2009**, *21*, 4181−4184.
(19) Yook, K. S.; Jang, S. E.; Jeon, S. O.; Lee, J. Y. *Adv. Mater.* **2010**, *22*, 4479−4483.
(20) So, F.; Krummacher, B.; Mathai, M. K.; Poplavskyy, D.; Choulis, S. A.; Choong, V.-E. *J. Appl. Phys.* **2007**, *102*, 091101.
(21) King, K. A.; Spellane, P. J.; Watts, R. J. *J. Am. Chem. Soc.* **1985**, *107*, 1431−1432.
(22) Laskar, I. R.; Hsu, S.-F.; Chen, T.-M. *Polyhedron* **2006**, *25*, 1167−1176.
(23) Hay, P. J. *J. Phys. Chem. A* **2002**, *106*, 1634−1641.
(24) Jankus, V.; Monkman, A. P. *Adv. Funct. Mater.* **2011**, *21*, 3350−3356.
(25) Kawamura, Y.; Brooks, J.; Brown, J. J.; Sasabe, H.; Adachi, C. *Phys. Rev. Lett.* **2006**, *96*, 017404.
(26) Adachi, C.; Kwong, R. C.; Djurovich, P.; Adamovich, V.; Baldo, M. A.; Thompson, M. E.; Forrest, S. R. *Appl. Phys. Lett.* **2001**, *79*, 2082−2084.
(27) Tao, S.; Lai, S. L.; Wu, C.; Ng, T. W.; Chan, M. Y.; Zhao, W.; Zhang, X. *Org. Electron.* **2011**, *12*, 2061−2064.
(28) Baranoff, E.; Curchod, B. F. E.; Monti, F.; Steimer, F.; Accorsi, G.; Tavernelli, I.; Rothlisberger, U.; Scopelliti, R.; Grätzel, M.; Nazeeruddin, M. K. *Inorg. Chem.* **2011**, *51*, 799−811.
(29) Zhou, Y.; Li, W.; Liu, Y.; Zeng, L.; Su, W.; Zhou, M. *Dalton Trans.* **2012**, *41*, 9373−9381.
(30) Chen, X.; Liao, J.-L.; Liang, Y.; Ahmed, M. O.; Tseng, H.-E.; Chen, S.-A. *J. Am. Chem. Soc.* **2003**, *125*, 636−637.
(31) Eom, S.-H.; Zheng, Y.; Wrzesniewski, E.; Lee, J.; Chopra, N.; So, F.; Xue, J. *Org. Electron.* **2009**, *10*, 686−691.
(32) Jou, J.-H.; Wang, W.-B.; Shen, S.-M.; S. Kumar, S.; Lai, I.-M.; Shyue, J.-J.; Lengvinaite, S.; Zostautiene, R.; Grigalevicius, J. V.; Chen, S.-Z.; Wu, C.-C. *J. Mater. Chem.* **2011**, *21*, 9546−9552.
(33) Zacharias, P.; Gather, M. C.; Rojahn, M.; Nuyken, O.; Meerholz, K. *Angew. Chem., Int. Ed.* **2007**, *46*, 4388−4392.
(34) Yang, X. H.; Jaiser, F.; Klinger, S.; Neher, D. *Appl. Phys. Lett.* **2006**, *88*, 021107.
(35) Mathai, M. K.; Choong, V.-E.; Choulis, S. A.; Krummacher, B.; So, F. *Appl. Phys. Lett.* **2006**, *88*, 243512.
(36) Wu, H.; Zou, J.; Liu, F.; Wang, L.; Mikhailovsky, A.; Bazan, G. C.; Yang, W.; Cao, Y. *Adv. Mater.* **2008**, *20*, 696−702.
(37) *Highly Efficient OLEDs with Phosphorescent Materials*; Yersin, H., Ed.; Wiley-VCH, Weinheim, 2008; Ch 8.
(38) Stöker, T.; Köhler, A.; Moos, R. *J. Polym. Sci., Part B: Polym. Phys.* **2012**, *50*, 976−983.
(39) Wu, H.; Zou, J.; Hu, D.; Liu, F.; Yang, W.; Peng, J.; Mikhailovsky, A.; Bazan, G. C.; Cao, Y. *Org. Electron.* **2009**, *10*, 1562−1570.